SYSTEMS, SCIENCE AND SOFTWARE

SSS-R-78-3421

IDENTIFICATION OF INDIVIDUAL EVENTS IN A MULTIPLE EXPLOSION FROM TELESEISMIC SHORT PERIOD BODY WAVE RECORDINGS

D. G. LAMBERT
T. C. BACHE

TOPICAL REPORT

SPONSORED BY
ADVANCED RESEARCH PROJECTS AGENCY
ARPA ORDER No. 2551

This research was supported by the Advanced Research Projects Agency of the Department of Defense and was monitored by AFTAC/VSC, Patrick Air Force Base, Flordia, 32925, under Contract No. F08606-76-C-0041.

OCTOBER 1977

P. O. BOX 1620, LA JOLLA, CALIFORNIA 92038, TELEPHONE (714) 453-0060

AFTAC Project Authorization No. VELA/T/7712/B/ETR

Program Code No. 6H189

Effective Date of Contract: October 1, 1976

Contract Expiration Date: September 30, 1978

Amount of Contract: $435,087

Contract No. F08606-76-C-0041

Principal Investigator and Phone No.
Dr. Thomas C. Bache, (714) 453-0060, Ext. 337

Project Scientist and Phone No.
Dr. Ralph W. Alewine, III, (202) 325-7581

UNCLASSIFIED

SECURITY CLASSIFICATION OF THIS PAGE (When Data Entered)

REPORT DOCUMENTATION PAGE

READ INSTRUCTIONS BEFORE COMPLETING FORM

1. REPORT NUMBER

2. GOVT ACCESSION NO.

3. RECIPIENT'S CATALOG NUMBER

4. TITLE (and Subtitle)

(6) IDENTIFICATION OF INDIVIDUAL EVENTS IN A MULTIPLE EXPLOSION FROM TELESEISMIC SHORT PERIOD BODY WAVE RECORDINGS.

(9) TYPE OF REPORT & PERIOD COVERED

Topical Report.

6. PERFORMING ORG. REPORT NUMBER

(14) SSS-R-78-3421

7. AUTHOR(s)

(10) D. G. Lambert, Thomas C. Bache
T. C. Bache

8. CONTRACT OR GRANT NUMBER(s)

(15) F08606-76-C-0041,
ARPA Order-2551

9. PERFORMING ORGANIZATION NAME AND ADDRESS

Systems, Science and Software
P. O. Box 1620
La Jolla, California 92038

10. PROGRAM ELEMENT, PROJECT, TASK AREA & WORK UNIT NUMBERS

Program Code No. 6H189
ARPA Order No. 2551

11. CONTROLLING OFFICE NAME AND ADDRESS

VELA Seismological Center
312 Montgomery Street
Alexandria, Virginia 22314

(11) 12. REPORT DATE

Oct [redacted] 77

13. NUMBER OF PAGES

40 (12) 48p.

14. MONITORING AGENCY NAME & ADDRESS (if different from Controlling Office)

15. SECURITY CLASS. (of this report)

Unclassified

15a. DECLASSIFICATION/DOWNGRADING SCHEDULE

16. DISTRIBUTION STATEMENT (of this Report)

Approved for public release, distribution unlimited.

17. DISTRIBUTION STATEMENT (of the abstract entered in Block 20, if different from Report)

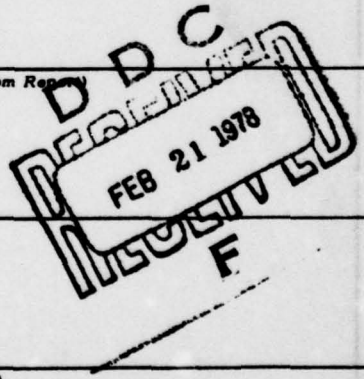

18. SUPPLEMENTARY NOTES

19. KEY WORDS (Continue on reverse side if necessary and identify by block number)

Seismology
Multiple Nuclear Explosions
Signal Analysis
Teleseismic Body Waves

20. ABSTRACT (Continue on reverse side if necessary and identify by block number)

The objective of this study is to detect and identify the individual events in a hypothetical multiple explosion. The data analyzed are simulated short period body wave recordings of that event. These were, presumably, constructed by lagging, scaling and summing a single event record according to some formula unknown to the analysts. Data for two stations,

388 507.

DD FORM 1 JAN 73 1473 EDITION OF 1 NOV 65 IS OBSOLETE

UNCLASSIFIED

SECURITY CLASSIFICATION OF THIS PAGE (When Data Entered)

20. Abstract (continued)

including both the single event and multiple event records, were provided to Systems, Science and Software by the VELA Seismological Center (VSC).

The data were analyzed by the MARS (Multiple Arrival Recognition System) program which uses a series of narrow-band filters to identify phase arrivals. Their amplitude and arrival time are accurately preserved. The variable frequency magnitude (VFM) discriminant is also computed and the multiple explosion records are clearly identified as being from an explosion.

For decomposition of the multiple event the MARS output for the single and multiple event records were cross-correlated. Two main groups of events separated by 6.7 to 7.8 seconds, depending on azimuth, were identified. Each of these groups appeared to include two or more explosions.

Subsequent comparison with the actual array configuration showed that the two main groups of events had been correctly identified. There were two events in each group and their lag times were correctly identified within 0.1 second. For these four events the relative amplitude estimates were correct within 10-20 percent. The actual array also included two other smaller and later events that were not identified by our analysis.

TABLE OF CONTENTS

LIST OF ILLUSTRATIONS

LIST OF ILLUSTRATIONS (continued)

LIST OF TABLES

I. INTRODUCTION AND SUMMARY

The objective of this study is to detect and identify the individual events in a hypothetical multiple explosion. The data are simulated far-field short period body wave recordings of that event. Seismograms were provided in digital form for two stations located about 19 and 91 degrees from the event and at azimuths of N127°W and N9°E. The two multiple event records were presumably constructed by lagging, scaling and summing a single event seismogram for the particular source region-receiver combination of interest. The single event record was also provided in digital form.

The signal analysis program called MARS (Multiple Arrival Recognition System) was used to decompose the multiple event. In this program the seismograms are filtered by a series of narrow-band filters to identify phase arrivals. The amplitude and arrival time (in a narrow frequency band) of the identified phases are accurately preserved.

A byproduct of the analysis is the variable frequency magnitude [$\bar{m}_b(f)$] for each seismogram. The $\bar{m}_b(f)$ values form the basis for a powerful earthquake/explosion discriminant (Savino and Archambeau, 1974). The first question addressed is, do the seismograms appear to be from an explosion? This question is addressed in Section III. We find that all four seismograms, the two single and the two multiple event records, are clearly recordings of an explosion event.

Decomposition of the multiple event record basically requires a cross-correlation of the pattern of phase arrivals in the single event records with those on the multiple event records. In Section IV we describe this analysis and give the results. The correlation is first done by eye and then is done automatically by cross-correlating the narrow-band filter output filter-by-filter and summing the resulting correlation functions.

Separation of event arrivals in far-field data is difficult because of the attenuation of high frequency energy in the records. We know from previous experience (Lambert, et al., 1977) that arrivals can generally be separated only when there is sufficient signal energy at frequencies greater than 3.5 times the inverse of the lag time between arrivals. Therefore, we know at the outset that events separated by times on the order of a second or less will be very difficult to detect.

The results are unambiguous in identifying two main groups of events separated by 6.7 or 7.8 seconds, depending on the station azimuth. The longer lag times are seen at ANMO (Δ = 91°), suggesting that the array is oriented more nearly in line with this station, or approximately north-south. Each of the two main groups seems to consist of two or more explosions. All the events identified by the automated cross-correlation or the cross-correlation by eye are summarized in Table 1. Also shown in the table are the relative amplitudes determined from the informal correlation and from the cross-correlation output.

Examining the table, we see that the first group of events consists of two or three explosions (1, 2 and 3 in the table). The lag times are about 0.1 seconds greater at MAIO than at ANMO suggesting that the three events proceed from south to north. The second group of explosions seems to consist of at least two events (4 and 5 in the table). The arrival times are 1.0 to 1.2 seconds earlier at MAIO than at ANMO. This suggests that the events in the second group are considerably south, 10 km or more, of those in the initial group.

Events 6 and 7 in Table 1 are identified in a very tentative way by the informal correlation. Their amplitudes are rather large. However, examining the cross-correlation functions (Figures 10 and 11 in Section 4.3), we see only a

TABLE 1

INDIVIDUAL EVENTS IN THE MULTIPLE EXPLOSION ARRAY

	ANMO				MAIO			
	Lag Time		Normalized Amplitude		Lag Time		Normalized Amplitude	
Event	Sec. 4.2*	Sec. 4.3**	Sec. 4.2*	Sec. 4.3**	Sec. 4.2*	Sec. 4.3**	Sec. 4.2*	Sec. 4.3**
1	0.0	0.0	0.5	0.45	0.0	0.0	0.4	0.35
2		0.4+		0.5+	0.51+		0.5+	
3	0.81		0.55		0.90	0.90	0.55	0.4
4	7.80	7.90	0.55	0.7	6.70	6.80	0.60	0.75
5	8.81	8.60+	0.8	0.35+	7.60	7.70	0.7	0.3
6	14.67+		0.9+		13.51+		0.8+	
7					21.31+		0.4+	

* Identified by correlation by eye.

** Identified by automated cross-correlation.

\+ Identification less certain than for the others.

hint of Event 6 and no indication of the presence of Event 7. The latter, we are fairly sure, is a misidentification (in the correlation by eye) that arises due to interfering phases from earlier events in the sequence. The Event 6 may or may not be present. Our best estimate is that it probably is not.

Comparison to the Correct Answers

After completing the first draft of the report which is summarized in the preceding paragraphs, we were provided with the correct answers. These are compared to our estimates in Section V. Briefly summarized, the results from the comparison are these. There were six events with relative amplitudes 0.4, 0.4, 0.8, 0.4, 0.2, respectively. Our automated cross-correlation correctly identified the first four of these with a maximum error in the lag time of less than 0.1 seconds. For these four our amplitude estimates were correct within 10-20 percent. The last two events were entirely missed, presumably because they are smaller.

We also ventured an estimate of the array orientation which can be compared to the actual orientation shown in Figure 13. As was thought, the first two events proceeded (generally) from south-to-north. Also, the first event in the second group is 12 km south of the last event in the first group, which is close to our estimate.

The best results were achieved with the automated cross-correlation, which is encouraging. The more arduous informal correlation misidentified several events and gave relatively poor estimates of the relative amplitudes. However, this method was helpful in guiding our thinking and in confirming the more abstract results from the automated cross-correlation.

II. DATA

The data used for this test consist of short-period vertical component recordings from stations ANMO and MAIO for two events. The first is a single explosion at the Soviet test site near Semipalatinsk. The second event is a synthetic multiple explosion constructed by scaling, lagging and summing the single event records. The four records (two for ANMO and two for MAIO) are shown in Figures 1 and 2. All data were provided by the SDAC in digital form with a sampling rate of 20 points per second. The station ANMO is about 91 degrees from Semipalatinsk at an azimuth of 9 degrees east from north. Station MAIO is at an epicentral distance of about 19 degrees and an azimuth of 233 degrees east from north. The two stations are therefore 136 degrees apart.

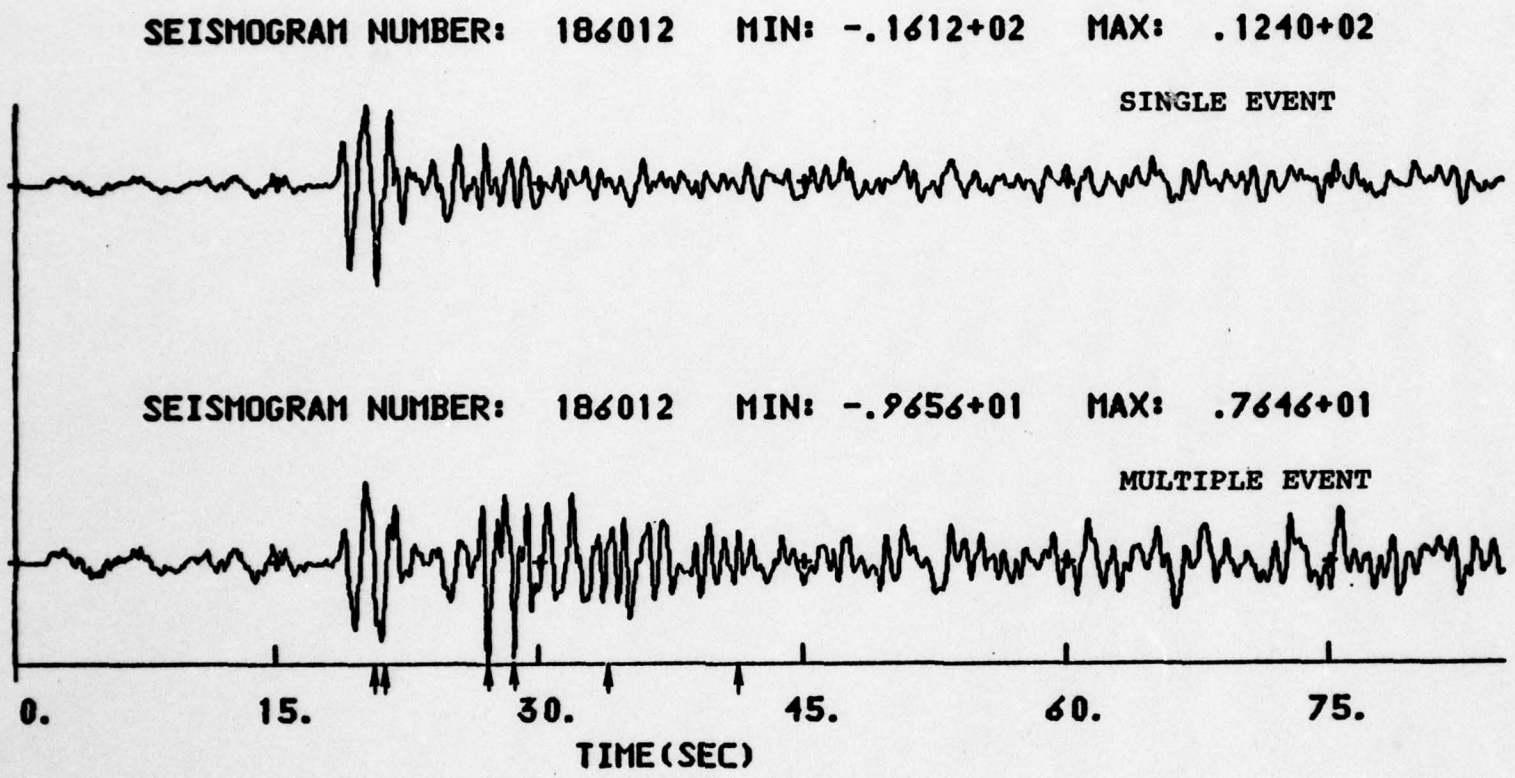

Figure 1. The data for Station ANMO are shown. The top record is for the single event and the multiple event record is plotted below.

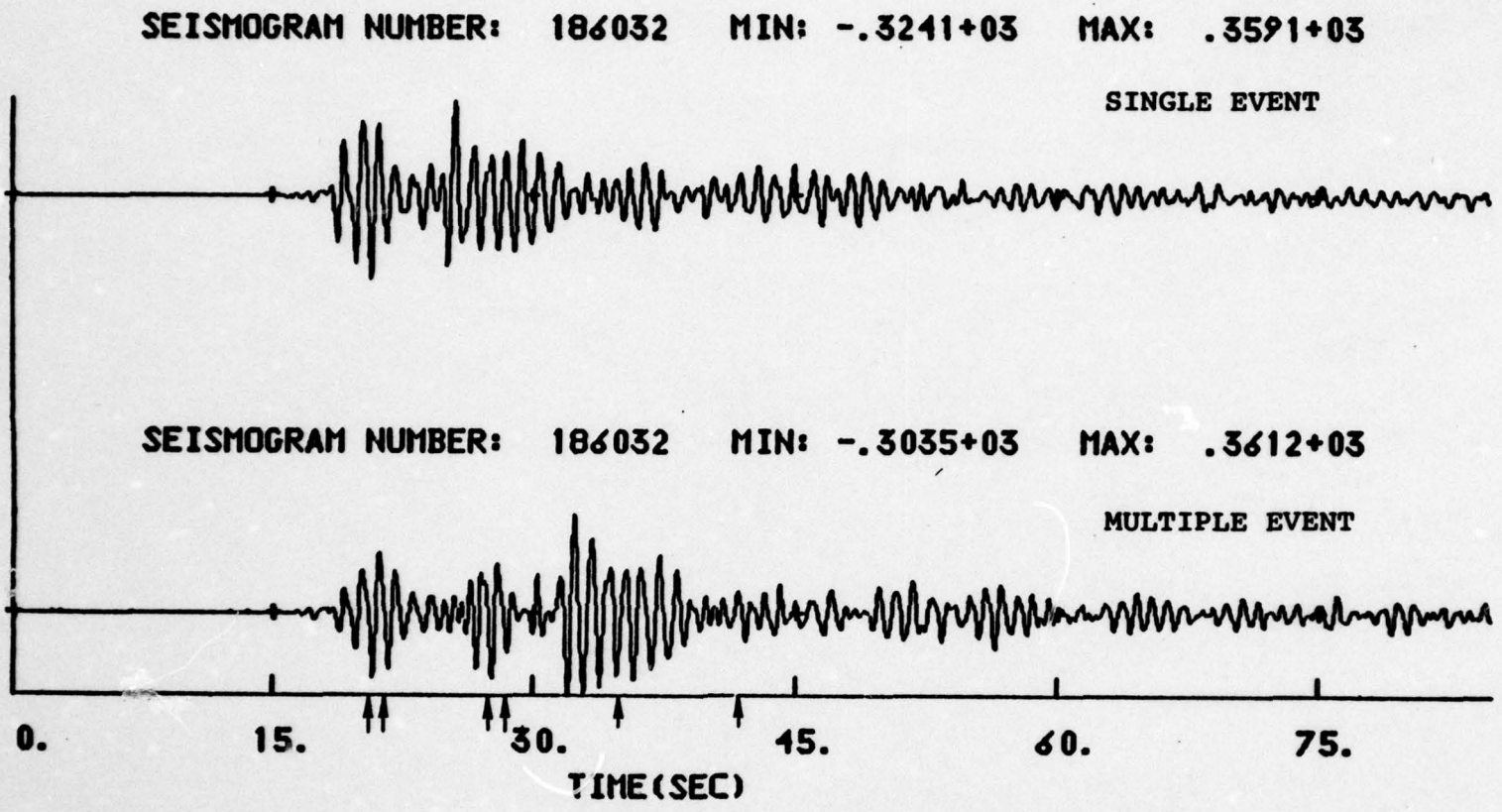

Figure 2. The data are shown for Station MAIO. The top record is for the single event and the multiple event record is plotted below.

III. EVENT IDENTIFICATION USING THE VARIABLE FREQUENCY MAGNITUDE

An obvious question one might ask about the simulated multiple explosion under study is, can the multiple explosion be clearly identified as an explosion event rather than an earthquake? Since the $\bar{m}_b(f)$ values used for the VFM (Variable Frequency Magnitude) discriminant (Savino and Archambeau, 1974) are byproducts of our narrow-band filter analysis, we can plot these values together with earthquake and explosion data previously analyzed.

In Figure 3 is shown a plot of $\bar{m}_b$ (0.45 Hz) versus $\bar{m}_b$ (2.25 Hz) for LASA recordings of shallow Eurasian earthquakes and presumed explosions. Also shown are the same quantities for several simulated multiple explosion seismograms that were constructed in much the same way as those being studied here (for a detailed description of Figure 3 see Chapter VI of Bache, et al., 1976). These earlier multiple explosion scenarios were specifically designed to appear earthquake-like in terms of the M_s-m_b, complexity and first motion discriminants. These simulated multiple explosions clearly separate from the shallow earthquakes to which they are compared in Figure 3.

The station ANMO is at a distance (≈91 degrees) from the Semipalatinsk event that is about the same as most of the events in the LASA data plotted in Figure 3. We plot the data from both the single event (Z) and the simulated multiple event (ZSUM) on Figure 3 and see that they are both clearly identified as explosions. We point out that we are uncertain of the static instrument gain for the records and it is possible that a scale factor should be added to all $\bar{m}_b(f)$ values, moving them along a 45 degree line.

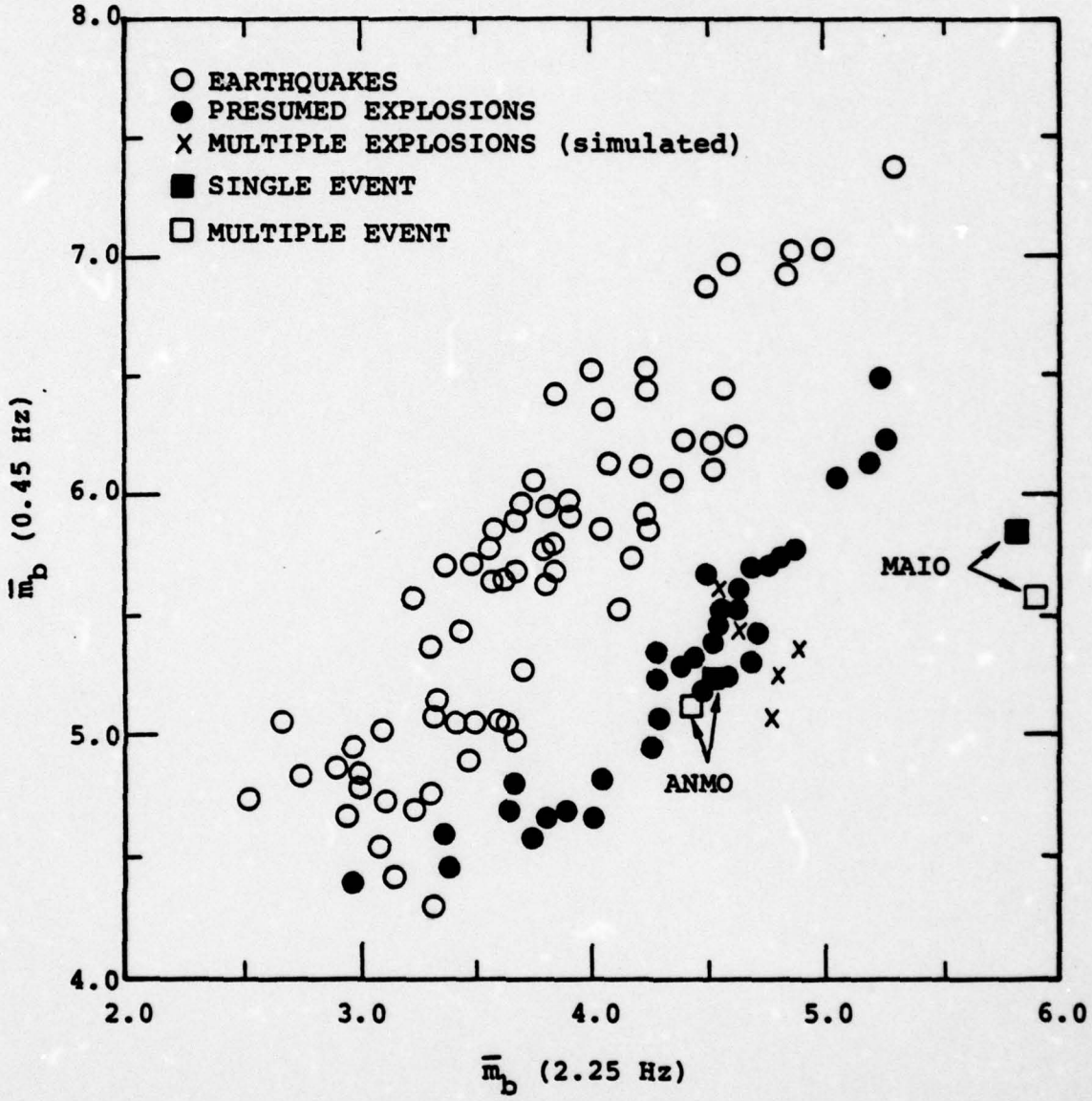

Figure 3. The variable frequency magnitude estimates [$\bar{m}_b(f)$] from the seismograms of Figures 1 and 2 are compared to those from a population of Eurasian earthquakes and presumed explosions recorded at LASA.

The $\bar{m}_b(f)$ values for station MAIO are also plotted on Figure 3 and fall well outside all other values. This is presumably because MAIO is at a much closer distance (≈19 degrees).

For a more reasonable comparison to the $\bar{m}_b(f)$ values for MAIO, we select a previously analyzed population of North American events recorded at the Canadian array YKA. These data are shown in Figure 4, together with the $\bar{m}_b(f)$ values from MAIO and ANMO. Since we do not know the static instrument gains, these values can move along a 45 degree line as indicated in the figure. Once again, both the single and multiple explosion events are clearly identified as explosions.

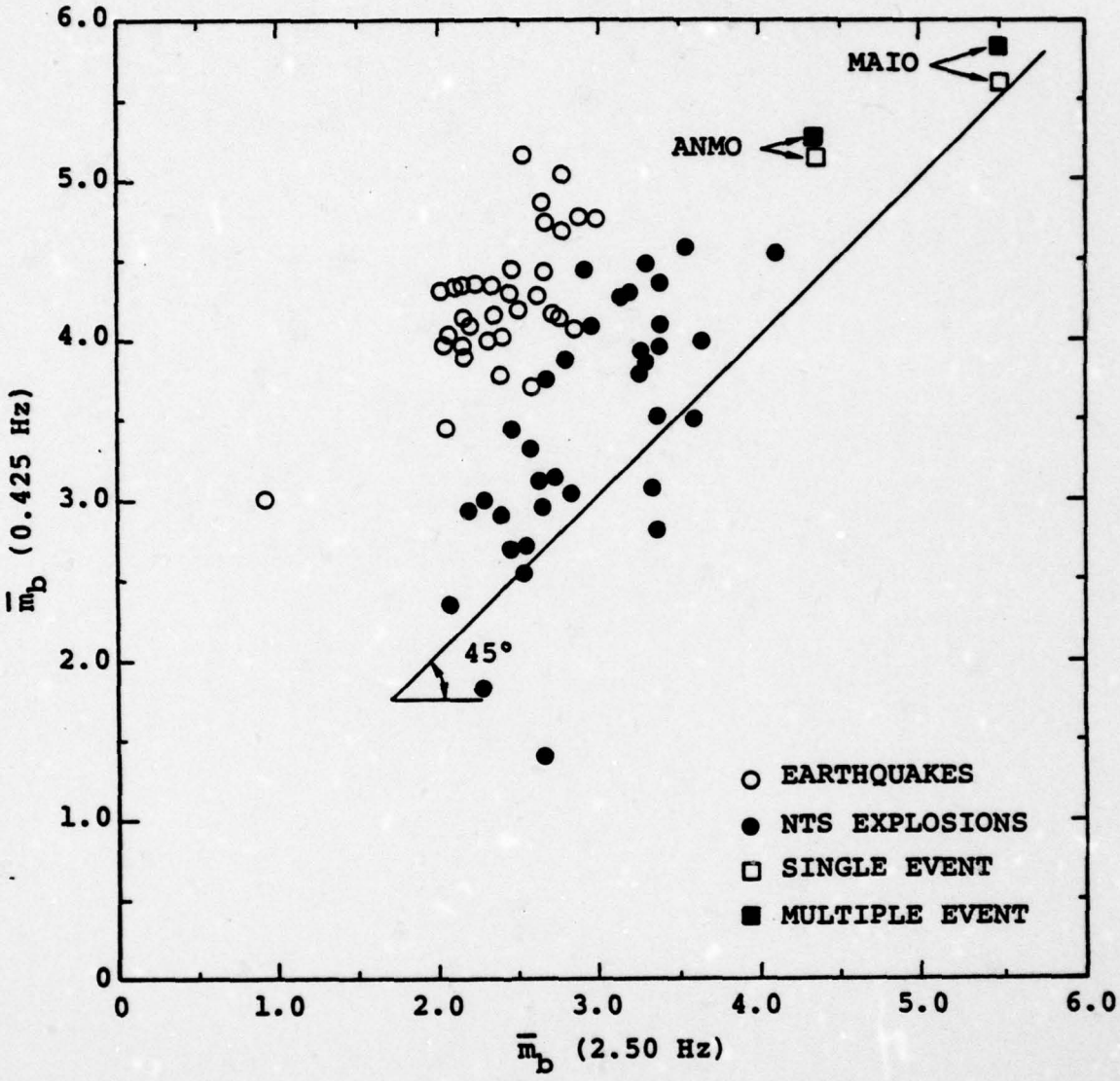

Figure 4. The variable frequency magnitude estimates from the seismograms of Figures 1 and 2 are compared to those from a population of Gulf of California earthquakes and NTS explosions recorded at YKA.

IV. DECOMPOSITION OF THE MULTIPLE EVENT

4.1 INTRODUCTION

The method used for identifying the individual events in a multiple explosion array was described in some detail in an earlier report (Lambert, et al., 1977). In the earlier work our attention was directed almost entirely to near-field data. In the current study we are concerned with recordings at large ranges (approximately 19 and 91 degrees) where the high frequency information has been greatly attenuated.

Briefly described, the method employed is as follows. Each seismogram to be analyzed is Fourier transformed and filtered by a narrow-band, Gaussian filter. The Hilbert transform of the filtered spectrum is then constructed and inverse-transformed to obtain the envelope function. The peaks of the envelope function indicate phase arrivals of energy in a narrow band of frequencies near the filter center frequency. The arrival times are accurately preserved by the times of these peaks. Further, the relative amplitudes of the peaks reflect the relative amplitudes of the arriving phases.

For the experiment which this report describes we have a multiple event record from two stations. These multiple event records are presumed to have been constructed by lagging, scaling and summing a single event record according to some formula based on the timing and spacing of the individual events in the hypothetical multiple explosion array. We also have been provided with the two single event records.

In order to decompose the multiple event record we do the following. All four records are filtered by narrow-band filters at series of center frequencies spanning the range at which spectral energy is present. Our task is to identify the arriving phases on the single event records and then to

correlate this pattern with the identified phase arrivals on the multiple event records to identify the repeated presence of the single event.

What are the constraints on this method? In our previous study (Lambert, et al., 1977), we found that we were able to separate individual arrivals whenever there was "sufficient" signal energy at frequencies greater than about 3.5 times the inverse of the lag time between these arriving signals. For teleseismic short period recordings this means that identifying events separated by less than a second can only be achieved if there is considerable signal energy at frequencies of 3.5 Hz and higher. Generally this is not the case.

Basically our problem is one of cross-correlation of a particular kind of output. In Section 4.2 we describe the results achieved by carrying out the cross-correlation by eye. While it may work best because of the opportunity to inject human judgement, this is certainly a slow and arduous way to proceed. Therefore, the cross-correlation was automated in a manner described in Section 4.3. The automated method worked very well and gives the best results. The informal correlation is described because of the insight it gives to the procedure.

4.2 IDENTIFICATION OF EVENTS

A series of twenty narrow-band filters with center frequencies ranging from 0.3 to 9.0 Hz were applied to the single and multiple event signals (Figures 1 and 2) from the stations MAIO and ANMO. A parameter of some minor importance is the filter Q or width. After several experiments, a value that seemed to be optimum was selected. The results were then plotted as shown in Figures 5 and 6. For each seismogram these are plots of the time of arrival of the largest envelope peaks versus the filter center frequency (f_c).

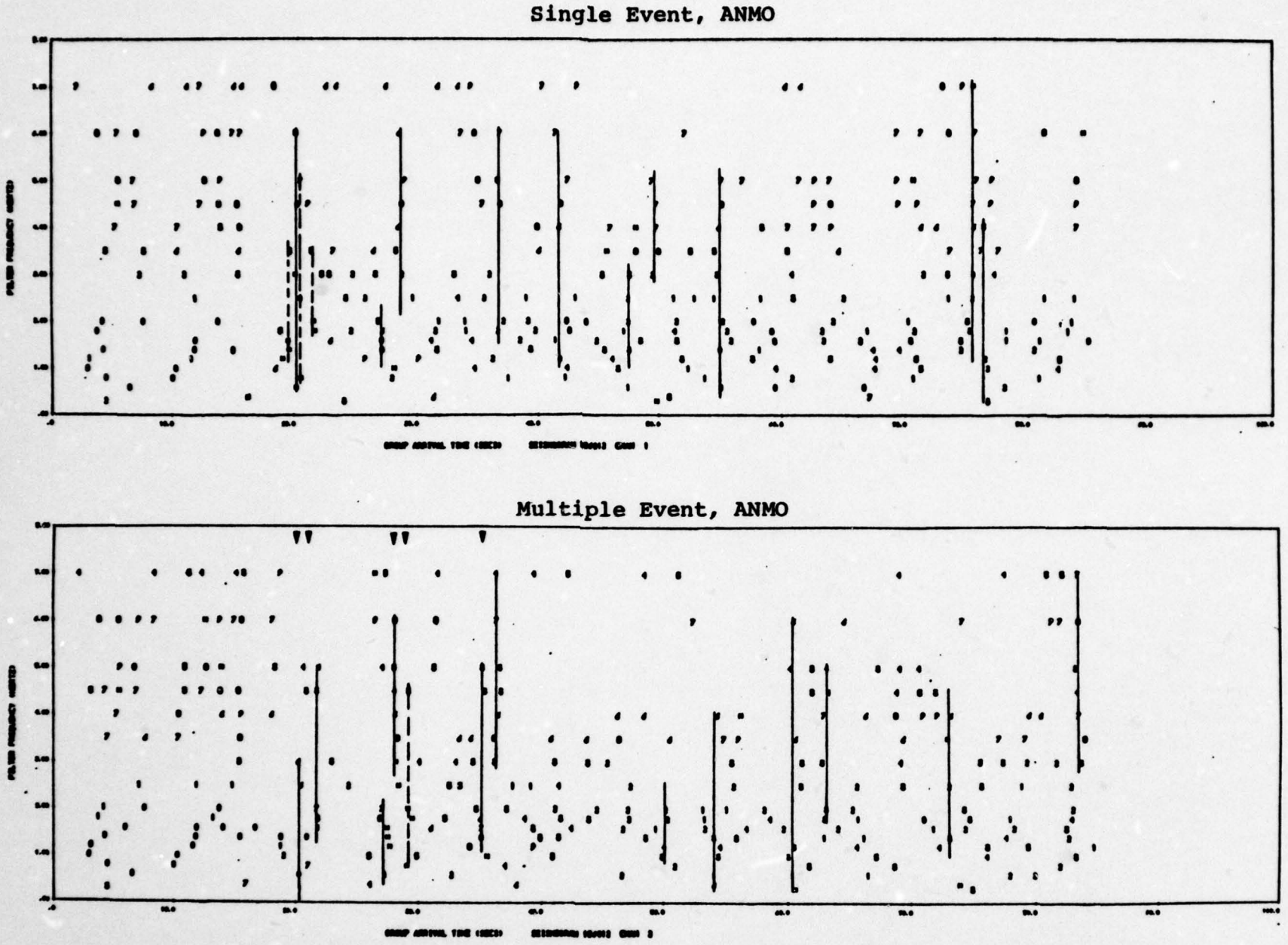

Figure 5. The relative peak amplitudes are plotted as functions of frequency and arrival time for Station ANMO. The plot for the single event record is on top with that for the multiple event below.

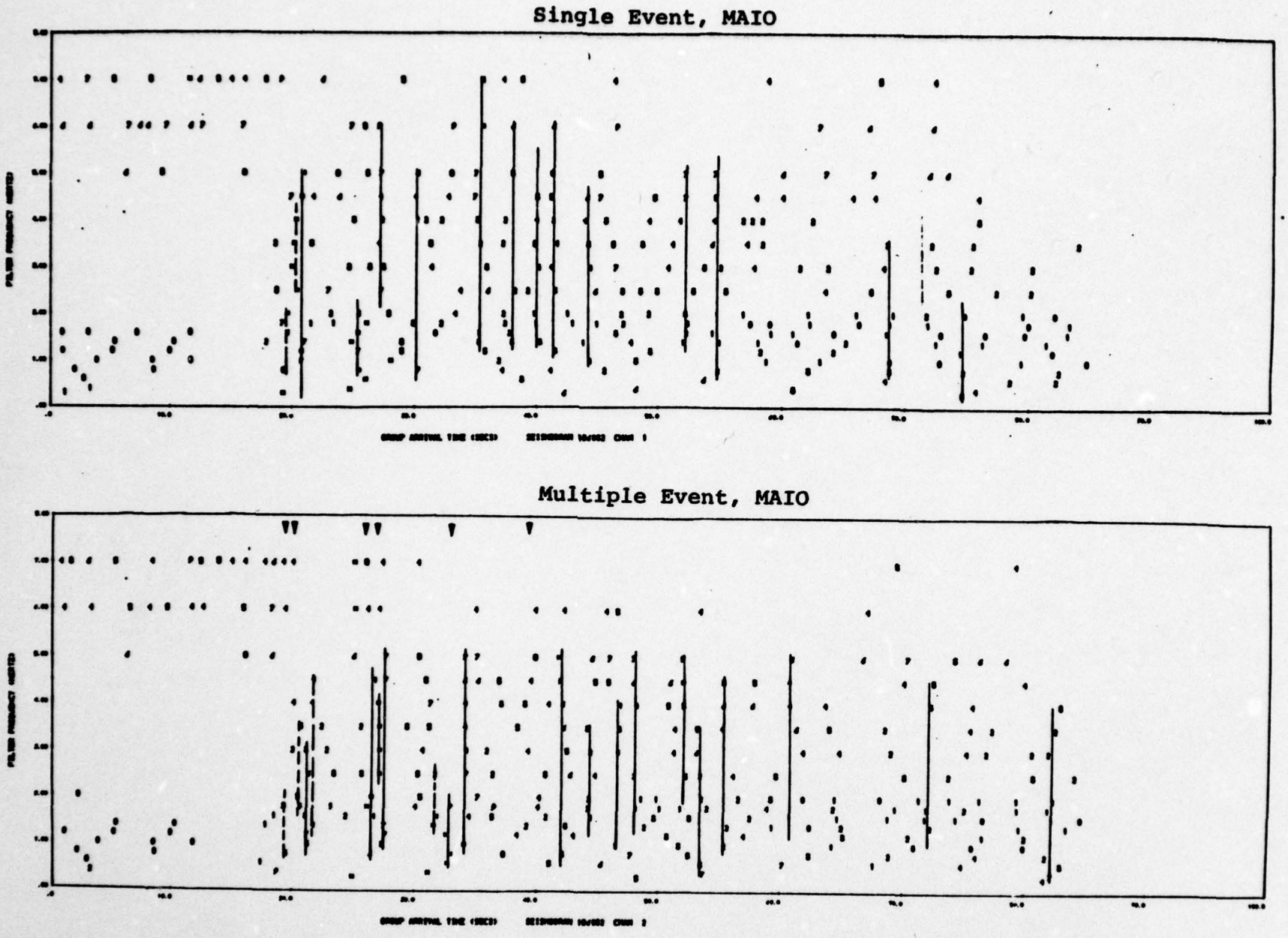

Figure 6. The relative peak amplitudes are plotted as functions of frequency and time for Station MAIO. The plot for the single event record is on top with that for the multiple event below.

For each f_c the plot symbols are numerals that indicate the relative amplitudes of the peaks compared to the largest for that frequency, which is indicated by an asterisk. A "9" indicates that the amplitude is greater than 90 percent of the largest, etc., down to "0" which indicates peaks with amplitudes from 1 percent to 10 percent of the largest.

The next step is to identify the nondispersed phase arrivals. These are arrivals for which there are envelope peaks of roughly the same relative size persisting over a band of frequencies. We began by identifying these by eye, a task that requires some judgement, but one that is necessary before attempting to automate the process. The results obtained by direct examination of the plots in Figures 5 and 6 are described in this section while a later Section (4.3) is devoted to the results from an automated analysis.

In Figures 5 and 6 solid lines are drawn through the major phase arrivals. The dashed lines indicate distinct arrivals that may be present but are less certainly identified.

To decompose the multiple event records the task is basically to cross-correlate the two pairs of single and multiple event records in Figures 5 and 6. For each we then have "single station" decompositions. The results from the two can then be compared to improve the resolution. However, a complication is that stations at different azimuths will generally not see the same lag times (recall from Section II that ANMO and MAIO are 136 degrees apart in azimuth).

For Station ANMO a comparison of the single and multiple event plots clearly indicates the presence of two major groups of events separated by 8 seconds. There are indications of at least two explosions in each group with the four identified events occurring at 0.0, 0.81, 7.80 and 8.81 seconds. There is a less certain indication of a later event separated by

14.67 seconds from the first, but this may be due to constructive interference of later arrivals from the first four events.

The Station MAIO is much closer to the source than ANMO (19 degrees versus 91 degrees) and therefore contains considerably more signal energy at high frequencies. This is apparent in the envelope peak plots for MAIO in Figure 6. Once again, the single and multiple event records are compared to discover repeated patterns. Individual events can tentatively be identified at 0.0, 0.51, 0.9, 6.7, 7.6, 13.5 and 21.3 seconds. The events at 0.51 and 7.6 seconds are relatively less clear than those at 0.0, 0.9 and 6.7 seconds. Those at 13.5 and 21.3 seconds may not be real but may appear due to interference from later arrivals associated with the earlier events.

To obtain additional confidence in our event decomposition, we compare results from the two stations. These are summarized in Table 2. In order to combine the information from the two stations, we must make some assumptions about the origin of the lag time between events. There are basically two ways for these lag times to arise. First, the explosions could be closely spaced, but detonated in some sequence. Second, the explosions could be detonated simultaneously and the lag time be due to them being varying distances from the receiver. However, at 91 degrees the $dT/d\Delta$ is about 4.7 seconds/degree and lag times of a second require differential path lengths of about 23 km. At 19 degrees the event separation per second of time lag is about 9 km. Therefore, it is likely that most of the time lag between events (certainly the larger lag times) is due to them being detonated in sequence.

Comparing the event arrival times in Table 2, we see three possible groups of events. Events 1, 2 and 3 at MAIO

TABLE 2

SUMMARY OF EVENT LAG TIMES

Identified Event	ANMO Lag Time (sec)	MAIO Lag Time (sec)
1	0.0*	0.0*
2		0.51*
3	0.81	0.90
4	7.80	6.70
5	8.81*	7.60*
6	14.67**	13.51**
7		21.31**

* Less correlation than those without asterisks.

** These correlations could be due to constructive interference from earlier events.

and 1 and 3 at ANMO comprise the first group. Lag time variations between stations of the order represented could easily be due to azimuthal effects. The second group of events are those indicated as Events 4 and 5. There is then a single event identified as 6 at both stations. Finally, there is the event at 21.31 on the MAIO record for which no corresponding arrival is seen at ANMO. This is probably a spurious event identification.

In summary, two groups of explosion events are clearly present, being separated in time by about 6 to 9 seconds. Actually, this is fairly clear from direct examination of the original seismograms (Figures 1 and 2). Each of the two main groups seems to be composed of two or more explosions with separation times on the order of a second. Finally, there may be at least one other event lagged some 5 to 6 seconds after the second group.

Small differences in lag times between events can potentially be used to ascertain the orientation of the multiple explosion array if we assume it to be linear. This subject is discussed in Section 4.5.

4.3 AUTOMATION OF EVENT IDENTIFICATION BY CROSS-CORRELATION

The event identification results of the previous section were obtained by a careful examination of the narrow-band filter output. While slow and arduous, this method gives maximum rein to human judgement and intuition. As was pointed out, the event identification process is essentially one of cross-correlation using the single- and multiple- event records. In this section we describe the results obtained when this process is automated.

The cross-correlation of two signals is defined by

$$c(t) = \frac{1}{2\pi} \int_{-\infty}^{\infty} F_1(\omega)\ F_2^*(\omega)\ e^{i\omega t}\ d\ \omega,$$

where $F_2^*(\omega)$ is the complex conjugate of the Fourier transform of $F_2(t)$. The cross-correlation results presented in this report are from an Systems, Science and Software (S^3) modified version of the program COLLAPSE (Alexander and Lambert, 1971).

To decompose the multiple event, one of the simplest things one could try would be to cross-correlate the time signals for the single and multiple events at each station. The results for Station MAIO are shown in Figure 7. Only the two main groups of events separated by about six seconds can be seen and even these are not indicated unambiguously. Elementary cross-correlation of the signals clearly gives insufficient resolution.

In view of our analysis of the data in Figures 5 and 6, a better way to proceed is to cross-correlate the narrow-band filter output. This is done filter-by-filter and the results are summed to give the final cross-correlation function. In Figures 8 and 9 we show the cross-correlation functions for each station for a selected set of center frequencies. For the individual filters only the two main groups of events are clearly identified at about 14 and 21 seconds into time signal. At this stage the narrow-band filter output cross-correlation gives results little better than those from direct cross-correlation of the seismograms (Figure 7). However, the results are considerably enhanced by summing the individual filter correlations.

In Figures 10 and 11 we show the final cross-correlation functions for ANMO and MAIO. This function is a sum of the correlation functions for the individual filters (Figures 8 and

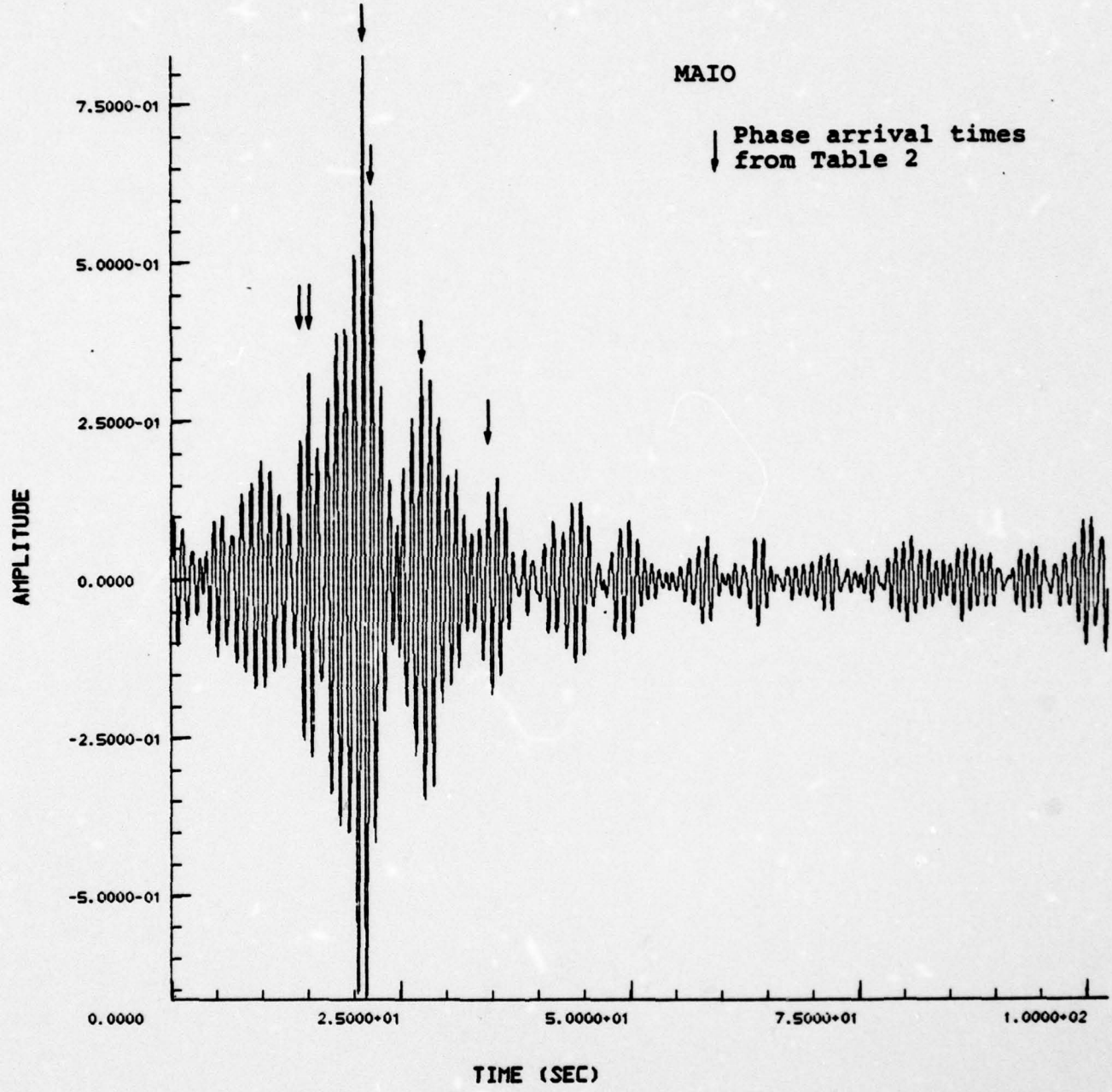

Figure 7. The cross-correlation function is plotted for direct correlation of the single and multiple event records for MAIO.

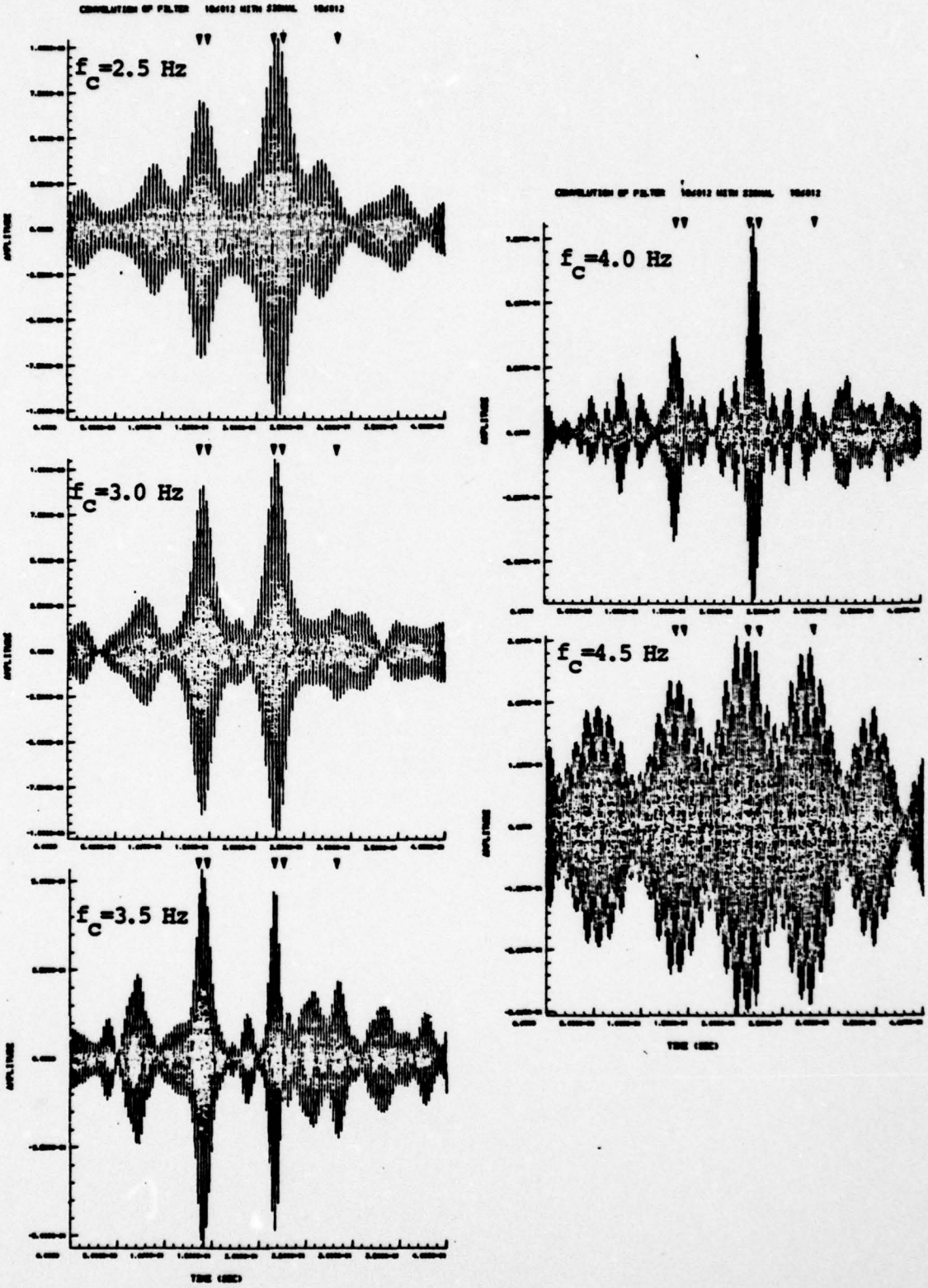

Figure 8. The ANMO cross-correlation functions are shown for correlation of the narrow-band filtered signals from the single and multiple events. The correlation is done filter-by-filter and the results are shown for five center frequencies (f_c). The phase arrival times from Table 2 are indicated on each plot.

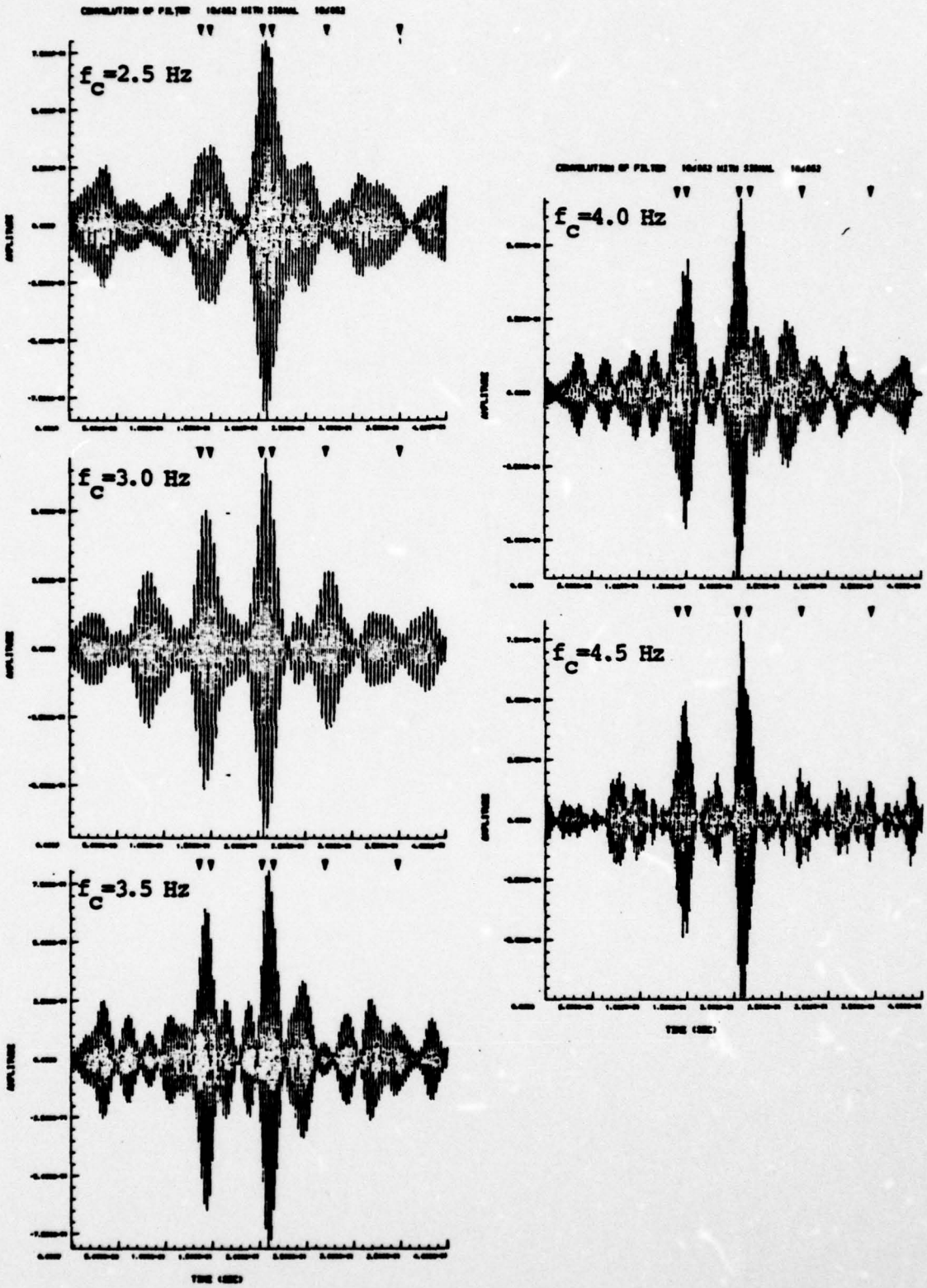

Figure 9. Results analogous to those in Figure 8 are shown for MAIO.

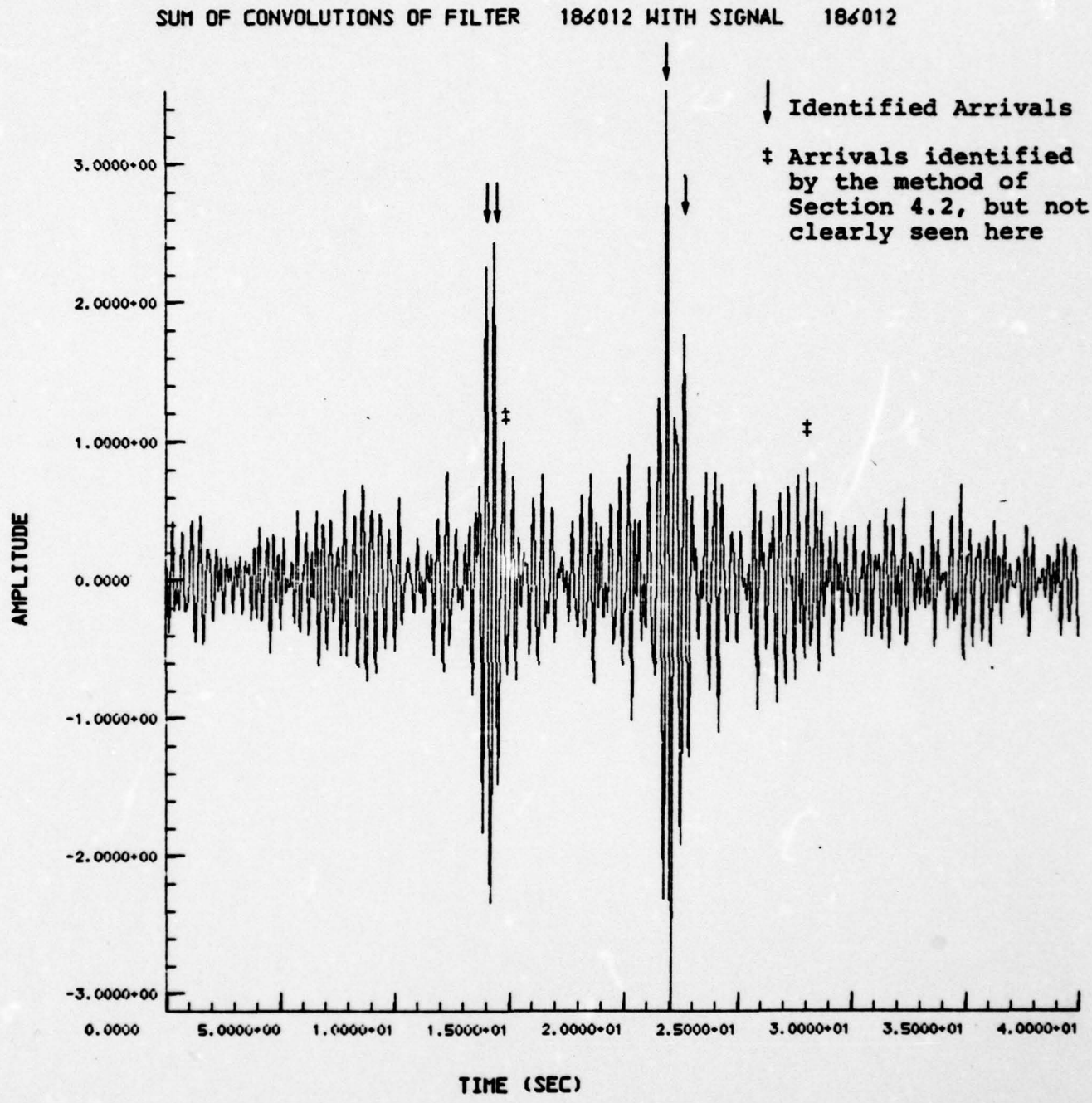

Figure 10. The summation of the cross-correlation functions of Figure 8 (ANMO) is shown. The four identifiable arrivals listed in Table 3 are indicated by arrows. Also indicated are the arrival times from Table 2 that do not correspond to identifiable peaks in the cross-correlation function.

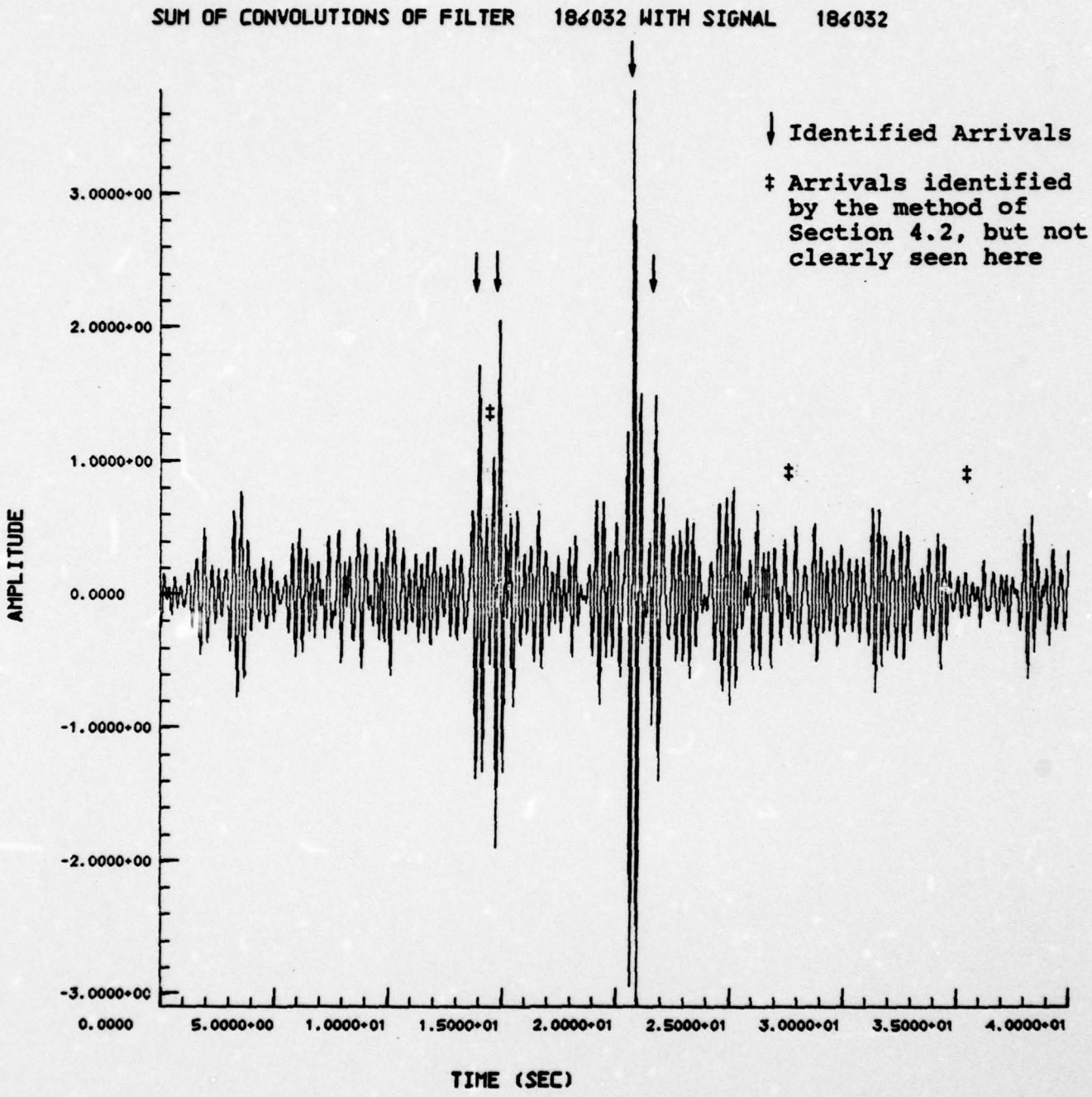

Figure 11. The cross-correlation function for MAIO is shown in the same form as that in the previous figure.

9). The answer depends to some extent on the selection of filters making up the sum. The particular combination shown seemed to be the best of those tried.

The individual event arrivals identified by the cross-correlation functions are indicated in Figures 10 and 11 and are tabulated in Table 3. Also summarized are the arrival times from the analysis of Section 4.2. For the four events in common, the cross-correlation results seem to agree rather well with those from direct examination of the narrow-band filter output. Taken together, the two give a more complete picture of the event.

We conclude that there are two main groups of events (1-3 and 4-5) separated by 6.7 to 7.8 seconds, depending on the azimuth. Each group consists of two or more events separated by lag times small enough to be at the limits of our resolving power. The cross-correlation functions seems to indicate that Event 7 is almost certainly not present and was misidentified by the analysis of Section 4.2. The Event 6 is difficult to judge. There is a hint of something in the cross-correlation function, but it is certainly very weak. Our best judgement is that this event is not present.

4.4 AMPLITUDE OF THE INDIVIDUAL EVENTS

As with the lag time determination, we now estimate the amplitude of the individual events with two different methods. We begin by using the data plotted in Figures 5 and 6. Each event arrival is identified by envelope peaks that arrive at the same time over a band of frequencies. The amplitude of each envelope peak accurately reflects the energy of the phase arrival at this frequency. A particular event arrival, say that at 27.5 seconds on the MAIO plot of

TABLE 3

SUMMARY OF EVENT LAG TIMES

	ANMO		MAIO	
Event	Lag Time from Table 2	Lag Time from Cross-Correlation	Lag Time from Table 2	Lag Time from Cross-Correlation
1	0.0	0.0	0.0	0.0
2		0.4*	0.51*	
3	0.81		0.90	0.90
4	7.80	7.90	6.70	6.80
5	8.81	8.60*	7.60	7.70
6	14.67*		13.51*	
7			21.31*	

* Identification less certain than for the others

Figure 6, is identified by peaks in several filters, five in this case. The corresponding peak in the single event record occurs at 20.8 seconds and is identified by the same five filters. A normalized amplitude can then be obtained by normalizing the corresponding peaks filter-by-filter and averaging the results. These are tabulated in Table 4.

The procedure described in the preceding paragraph requires considerable effort. However, if we analyze our procedure for obtaining the summed cross-correlation functions shown in Figures 10 and 11, we see that a similar normalization is a natural and automatic result of the analysis. In particular, the amplitudes of the peaks of the summed cross-correlation functions (divided by the number of filters) give the amplitudes relative to that of the single event used in the cross-correlation. These are read directly from Figures 10 and 11 and are tabulated in Table 4.

Because of the mixing of signals from the events, one cannot say much more about the amplitudes in Table 4 than that they provide indications of the relative yields. Recall that Events 1, 3, 4 and 5 were identified by both methods and it is these four events in which we have the most confidence. We tend to think that 6 and 7 are not real events, but appear due to constructive interference between later phase arrivals from the earlier explosions. However, we note that the analysis of Figures 5 and 6 assigns large amplitudes to these events even though they cannot be seen on the cross-correlation plots.

4.5 ORIENTATION OF THE ARRAY

If the array is assumed to be linear, its orientation can, in principle, be deduced from azimuthal variations in the differential travel times between events. The event lag times in which we have the most confidence are between the first and third events listed in Table 3. The lag time is about 1.1 seconds longer to ANMO (azimuth N9°E) than to MAIO

TABLE 4

NORMALIZED AMPLITUDES OF THE INDIVIDUAL EVENTS
IN THE MULTIPLE EXPLOSION ARRAY

	ANMO		MAIO	
Event+	Amplitudes from Figures 5 & 6	Amplitudes from Cross-Correlation, Figures 10 & 11	Amplitudes from Figures 5 & 6	Amplitudes from Cross-Correlation, Figures 10 & 11
1	0.5	0.45	0.4	0.35
2		0.5*	0.5*	
3	0.55		0.55	0.4
4	0.55	0.70	0.60	0.75
5	0.8	0.35*	0.7	0.3
6	0.9*		0.8*	
7			0.4*	

+ Event designation from Table 3.

* Identification less certain than for the others.

(azimuth N127°W). Since the $d\Delta/dT$ is about 23 km/sec at ANMO versus 9 km/sec at MAIO, a linear array in line with ANMO requires the smallest shot separation consistent with these lag times.

If any two events were known to have occurred simultaneously and the differential lag times were known exactly, we could fix the array orientation. However, the lag times we have determined are uncertain by a few tenths of a second (see the comparison in Table 3) and it is differences of this order that are indicative of the orientation. Further, since the events may occur in sequence, the problem is underdetermined with two stations. That is, for any pair of stations recording a pair of events we can write the set of equations

$$t_1 = p_1 D \cos \phi_1 + T_o ,$$

$$t_2 = p_2 D \cos \phi_2 + T_o ,$$

$$\phi_2 - \phi_1 = \Delta\theta ,$$

where t_1 and t_2 are the lag times perceived at Stations 1 and 2, p_1 and p_2 are the ray parameters for these stations, T_o is the detonation lag time and the other quantities are defined in Figure 12. These are three equations in the four unknowns T_o, D, ϕ_1 and ϕ_2. If the events were detonated simultaneously ($T_o = 0$), these can be solved. For $T_o \neq 0$ a third station is sufficient to uniquely determine the solution. This, of course, assumes no errors in the lag times. If errors are present, more stations are needed so a best fitting solution to an overdetermined set of equations can be constructed.

If the events are in a linear array, it doesn't matter how many there are. Each additional event adds two equations like the first two listed above and two unknowns, the detonation lag time and the separation. Therefore, three stations are, in principle, enough to uniquely determine the orientation of the array.

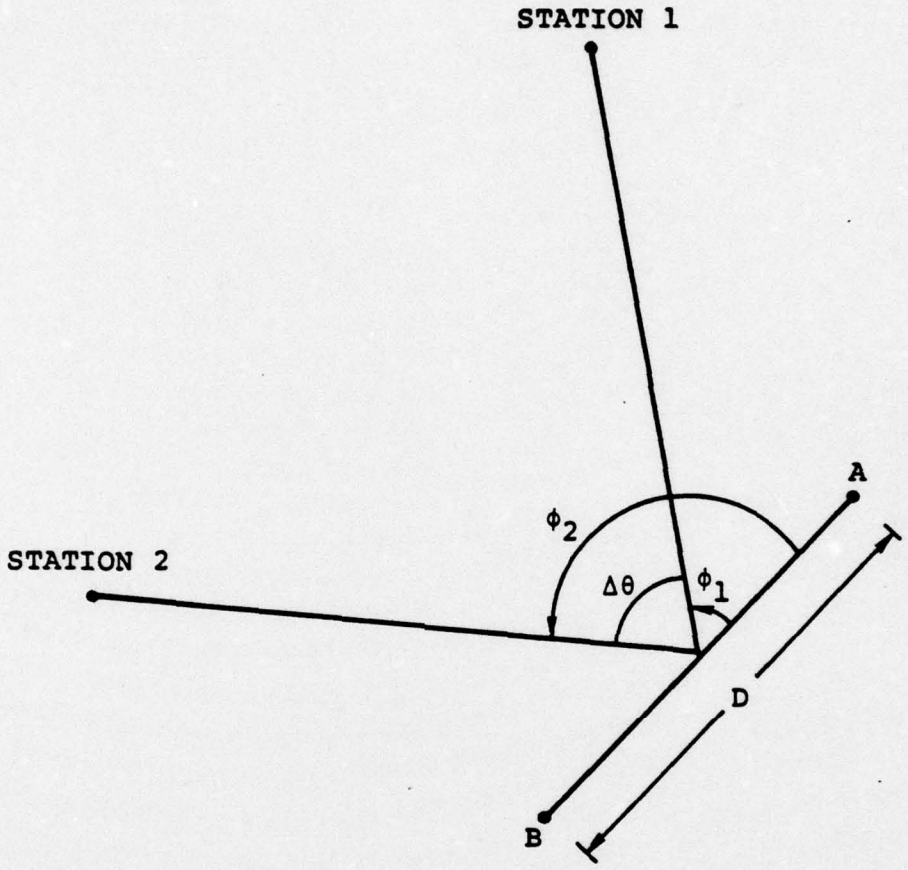

Figure 12. The geometry is shown for two stations recording two events detonated in sequence, first A, then B.

V. COMPARISON TO ACTUAL ARRAY CONFIGURATION

After completing the analysis described in Section IV, the details of the actual array configuration were provided for comparison to our answers (Captain M. J. Shore, personal communication). There were six events in a linear array oriented N45°W. The detonation sequence and event spacing are shown schematically in Figure 13.

The multiple event records were constructed by lagging, scaling and summing individual event records at the two stations. It is the time lag and relative size of events on each record that we determined in our analysis. The actual numbers used to construct the seismograms are summarized in Table 5.

Before comparing the actual values to those deduced in Section IV, we make some comments about the time lags in Table 5. The equations relating the time lags to the array configuration are given in Section 4.5. If we use the station locations (distance, azimuth with respect to the event) given in this report, the time lags in Table 5 are inconsistent with the array configuration, though the deviation is small. Therefore, the distances and azimuths used for computing the actual lags must have been different than those mentioned in this report.

The actual and computed lag times and relative amplitudes are compared in Tables 6 and 7. As might have been expected, the lag times from the automated cross-correlation of Section 4.3 are the most accurate. With this method we correctly identified Events 1, 2, 3 and 4 at both stations with the lag time error being less than 0.1 seconds in every instance. The Events 5 and 6 are relatively small and were not identified by our analysis.

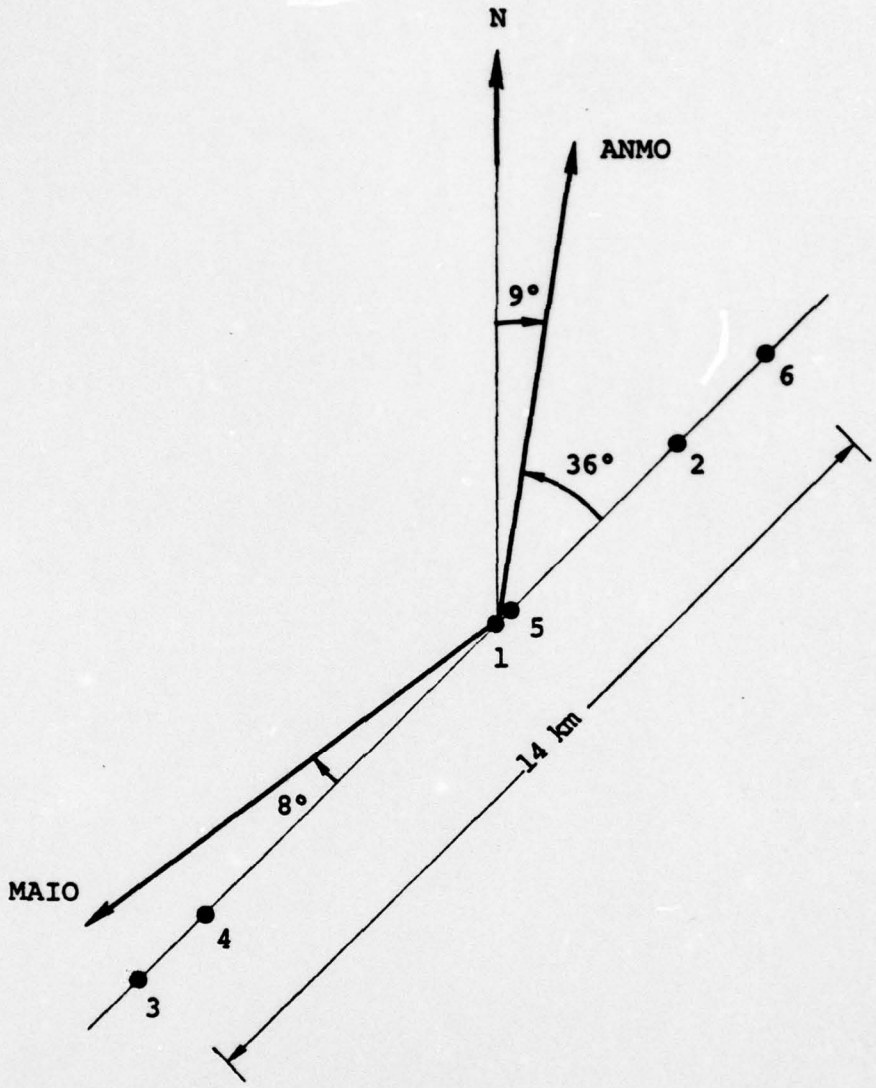

Figure 13. The actual array configuration is shown.

TABLE 5

DATA FOR CONSTRUCTION OF MULTIPLE EVENT SEISMOGRAMS
(from Capt. M. J. Shore, Personal Communication)

Event	Spacing from 1 (km)	Relative Amplitude	ANMO Time Lag (sec)	MAIO Time Lag (sec)
1	0.0	0.4	0.0	0.0
2	4.0	0.4	0.38	0.94
3	-8.0	0.8	7.94	6.82
4	-6.5	0.4	8.69	7.79
5	0.25	0.2	10.49	10.53
6	6.0	0.2	10.32	11.16

TABLE 6

COMPARISON OF ACTUAL AND COMPUTED DATA FOR ANMO

Actual Event	Actual Lag Time	Lag Time from Table 2	Lag Time from Cross-Correlation	Actual Amplitude	Amplitudes from Table 4 Figures 5 & 6	Amplitudes from Table 4 Cross-Correlation	Our Event No.
1	0.0	0.0	0.0	0.4	0.5	0.45	1
2	0.38		0.4*	0.4		0.5	2
		0.81			0.55		3
3	7.94	7.80	7.90	0.8	0.55	0.7	4
4	8.69	8.81	8.60*	0.4	0.8	0.35	5
5	10.49			0.2			
6	10.32			0.2			
		14.67*			0.9		6

* Identification less certain than for the others.

TABLE 7

COMPARISON OF ACTUAL AND COMPUTED DATA FOR MAIO

Actual Event	Actual Lag Time	Lag Time from Table 2	Lag Time from Cross-Correlation	Actual Amplitude	Amplitudes from Table 4 Figures 5 & 6	Amplitudes from Table 4 Cross-Correlation	Our Event No.
1	0.0	0.0	0.0	0.4	0.4	0.35	1
		0.51*			0.5		2
2	0.94	0.90	0.90	0.4	0.55	0.4	3
3	6.82	6.70	6.80	0.8	0.6	0.75	4
4	7.79	7.60	7.70	0.4	0.7	0.3	5
5	10.53			0.2			
6	11.16			0.2			
		13.51*			0.8		6
		21.31*			0.4		7

* Identification less certain than for the others.

The two summations of the cross-correlation functions shown in Figures 10 and 11 are repeated in Figures 14 and 15 with the correct event lag times indicated. On the ANMO summation in Figure 14 there is no indication of Events 5 and 6. However, at MAIO there is some peaking in the cross-correlation function at the arrival time for Events 5 and 6. If there were some other reason to suspect the presence of events with this lag time, this peaking would offer some corroborative evidence.

The actual and computed relative amplitudes are also compared in Tables 6 and 7. Once again, the automated cross-correlation technique gives much better results. In fact, if we average the relative amplitudes from the two stations for the four events correctly identified, we get 0.4, 0.45, 0.73, 0.33, which are within 10-20 percent of the correct values (0.4, 0.4, 0.8, 0.4).

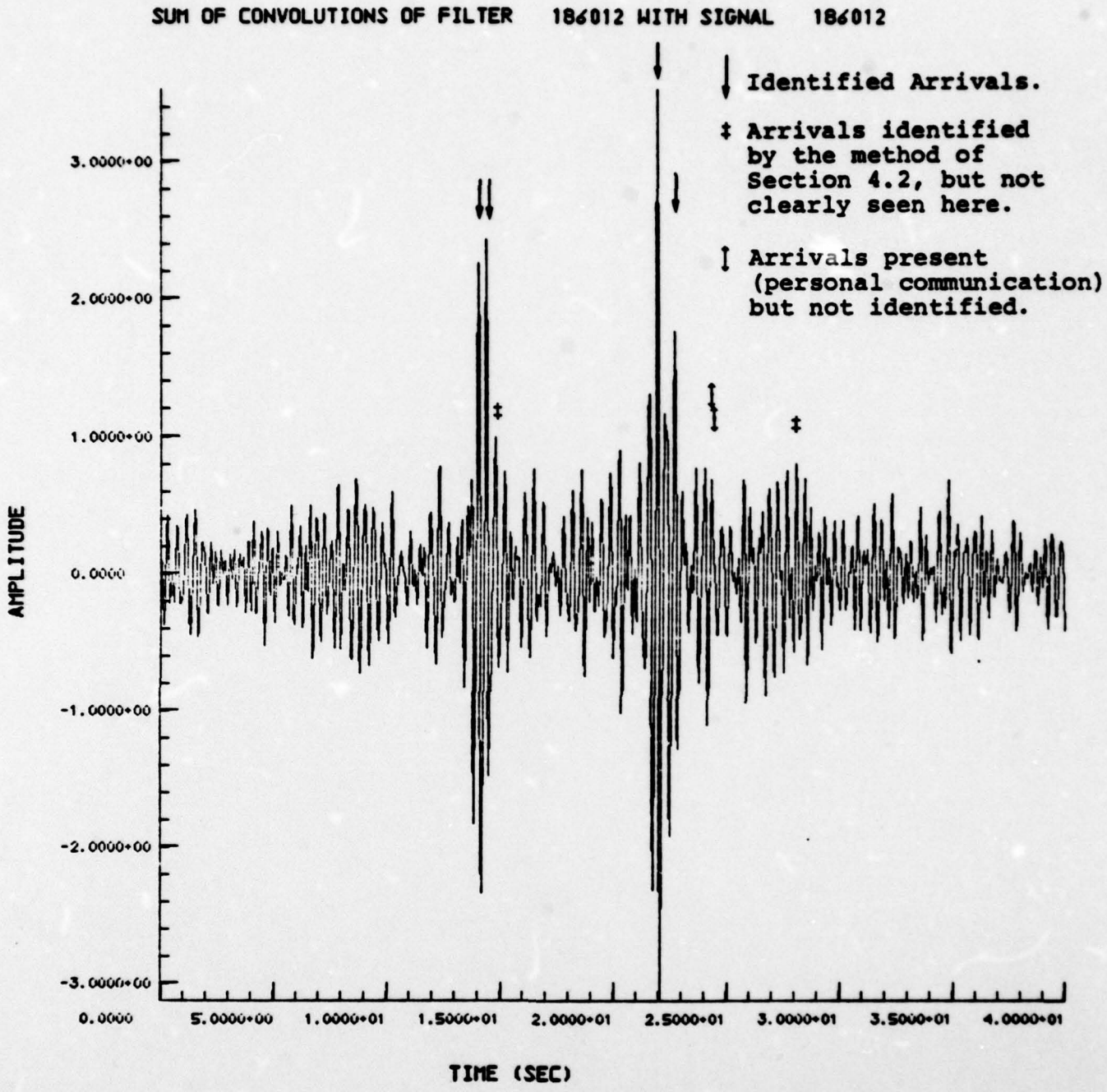

Figure 14. The summation of the cross-correlation functions of Figure 8 (ANMO) is shown. The four identifiable arrivals listed in Table 3 are indicated by arrows. We indicated the arrival times from Table 2 that do not correspond to identifiable peaks in the cross-correlation function and also those that are actually present (Personal Communication, 1977) but not identified.

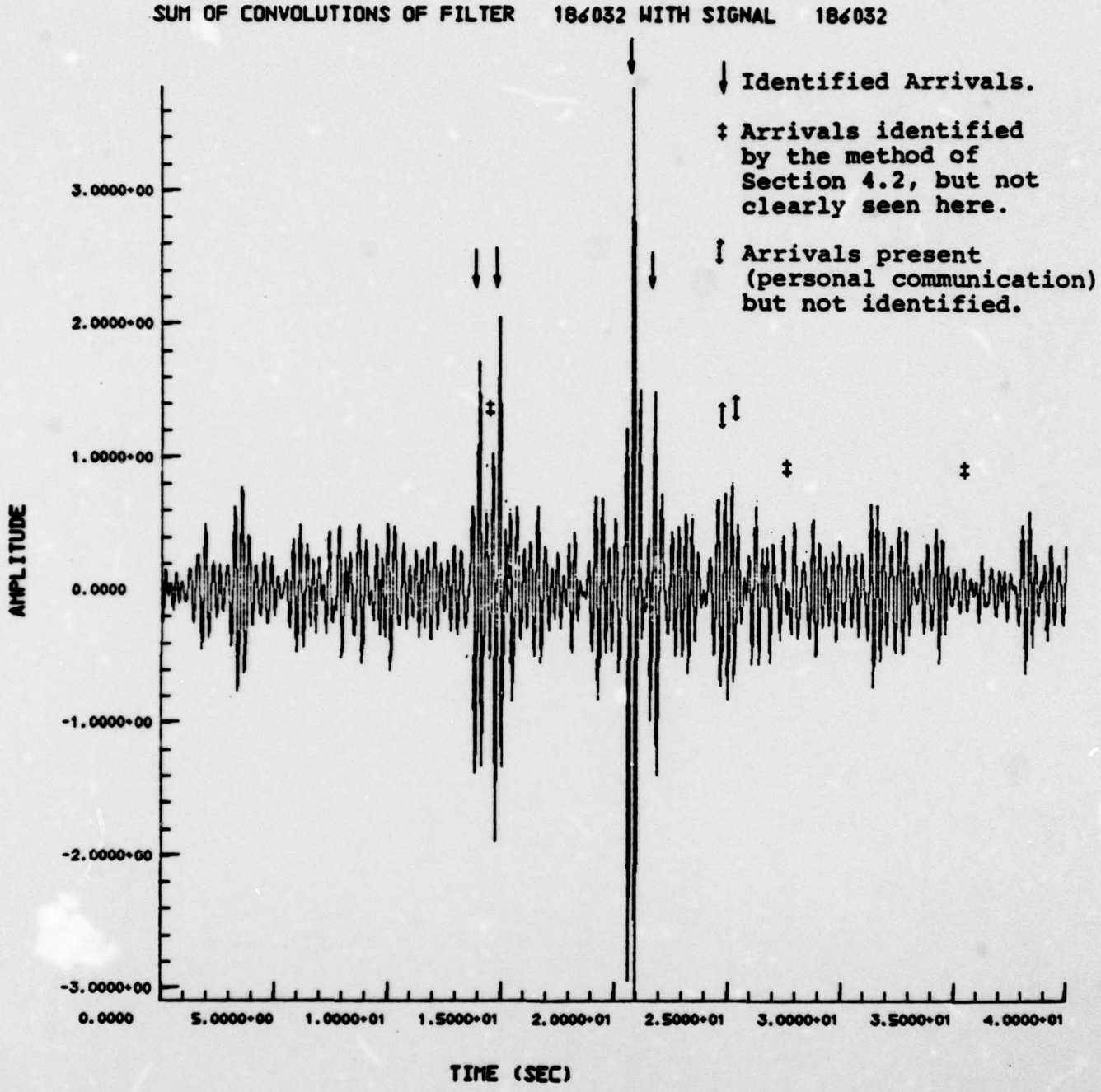

Figure 15. The cross-correlation function for MAIO is shown in the same form as that in the previous figure.

REFERENCES

Alexander, S. S. and J. W. Lambert, (1971), "Single Station and Array Methods for Improved Surface Wave Spectral Estimates," Teledyne Geotech Alexandria Laboratories, Report No. 264, AFTAC/VSC, 13 December 1971.

Bache, T. C., J. T. Cherry, D. G. Lambert, J. F. Masso and J. M. Savino, (1976), "A Deterministic Methology for Discriminating Between Earthquakes and Underground Nuclear Explosions," Systems, Science and Software Final Report, SSS-R-76-2925, July 1976.

Lambert, D. G., T. C. Bache and J. M. Savino, (1977), "Simulation and Decomposition of Multiple Explosions," Systems, Science and Software Topical Report, AFTAC/VSC, SSS-R-77-3194, June 1977.

Savino, J. M. and C. B. Archambeau, (1974), "Discrimination of Earthquakes from Single and Multiple Explosions Using Spectrally Defined Event Magnitudes," Trans. Amer. Geophys. Union, EOS (Abstract), 56, 1148.